

# Optimizing Breast Cancer Detection in Mammograms: A Comprehensive Study of Transfer Learning, Resolution Reduction, and Multi-View Classification

Daniel G. P. Petrini, Hae Yong Kim

**Abstract**—This study explores open questions in the application of machine learning for breast cancer detection in mammograms. Current approaches often employ a two-stage transfer learning process: first, adapting a backbone model trained on natural images to develop a patch classifier, which is then used to create a single-view whole-image classifier. Additionally, many studies leverage both mammographic views to enhance model performance. In this work, we systematically investigate five key questions: (1) Is the intermediate patch classifier essential for optimal performance? (2) Do backbone models that excel in natural image classification consistently outperform others on mammograms? (3) When reducing mammogram resolution for GPU processing, does the “learn-to-resize” technique outperform conventional methods? (4) Does incorporating both mammographic views in a two-view classifier significantly improve detection accuracy? (5) How do these findings vary when analyzing low-quality versus high-quality mammograms? By addressing these questions, we developed models that outperform previous results for both single-view and two-view classifiers. Our findings provide insights into model architecture and transfer learning strategies contributing to more accurate and efficient mammogram analysis.

**Index Terms**—Breast cancer detection, convolutional neural networks, deep learning, mammography, medical image analysis, multi-view classification, transfer learning.

## I. INTRODUCTION

**B**REAST cancer is the most common cancer among women globally, representing 23.76% of all new cancer cases diagnosed in 2022 [1]. Mammography, an X-ray-based imaging technique, is one of the most critical tools for early detection of the disease. To minimize error rates, mammograms should be interpreted by experienced radiologists, often supported by computer-aided detection and diagnosis (CAD) systems.

D.G.P. Petrini is with the Department of Electronic Systems Engineering, Polytechnic School, University of São Paulo, Brazil. (e-mail: dpetrini@usp.br, dpetrini@alumni.usp.br).

H.Y. Kim is with the Department of Electronic Systems Engineering, Polytechnic School, University of São Paulo, Brazil. (e-mail: hae.kim@usp.br).

## II. LITERATURE REVIEW

CAD systems based on neural networks have been proposed for single-view mammogram analysis. For instance, Shen et al. [2] first train a patch-based classifier and then reuse its weights to train a full-image classifier. Shu et al. [3] introduced novel pooling techniques to enhance performance, while Wei et al. [4] proposed a morphing technique to resize mammograms for input into a ResNet [5] backbone with ImageNet pre-trained weights.

On the other hand, multi-view systems aim to improve performance by processing more than one view simultaneously. Approaches vary significantly: McKinney et al. [6] developed a system that outperformed radiologists using private datasets. Petrini et al. [7] proposed a two-view classifier that fuses CC (cranio-caudal) and MLO (mediolateral-oblique) features through 2D concatenation for convolutional processing, following the training of a patch-based and single-view classifier. Chen et al. [8] process global and local features from both views, extracted using a backbone network, for subsequent classification. Nguyen et al. [9] aggregate view features using operations like averaging and concatenation, followed by processing in a fully connected network. Sarker et al. [10] introduced a SwinTransformers-based approach that integrates self-attention and cross-attention mechanisms for breast mass lesion classification.

## III. METHODOLOGY

After analyzing multi-view mammogram classification approaches, we formulated the following key questions:

- 1) *Is the patch classifier necessary?* Shen et al. [2] and Petrini et al. [7] incorporated a patch classifier as an intermediate step in the transfer learning process. Is this step truly essential?
- 2) *What is the most suitable backbone for mammogram classification?* Do backbone models that perform well on ImageNet classification also achieve better results on mammograms? Are models trained on ImageNet with a larger dataset (21k or 22k categories) superior to those trained on the smaller dataset (1k categories)? Do models with higher input image resolutions yield better performance for mammogram classification?

- 3) *Can mammogram resolution be reduced without significantly affecting classification performance?* Lower-resolution mammograms reduce computational resource requirements for processing. One promising approach is the “learn-to-resize” technique [11], which adaptively optimizes resizing for specific tasks. How effective is this method when applied to mammogram classification?
- 4) *Does the two-view classifier provide a significant performance improvement over the single-view classifier?* A two-view classifier cannot be directly compared to a single-view classifier, as the former produces  $n$  results for a dataset with  $2n$  images, while the latter generates  $2n$  results. To ensure a fair comparison, we combined the results of the single-view classifier applied to each mammographic view (CC and MLO) using both average and maximum operations, reducing the output to  $n$  results.
- 5) *How does image quality affect the answers to the above questions?* These questions can be explored using both low-quality analog mammograms (such as CBIS-DDSM [12]) and high-quality digital mammograms (such as VinDr-Mammo [13]). Would the answers differ depending on the quality of the mammographic images?

By investigating these questions, we aim to refine best practices in machine learning-based mammogram classification, optimizing both accuracy and computational efficiency. In doing so, we developed models that surpass previous results for both single-view and two-view classifiers on the CBIS-DDSM dataset. To select the base model architectures, we will follow an evolutionary scale starting from ResNet [5] until ConvNeXt [14], using open source implementations from Wightman [15] and from PyTorch<sup>1</sup>. We will use only publicly available mammogram datasets. Our source code and models are available online<sup>2</sup>.

#### IV. ARCHITECTURE EXPLORATION IN CBIS-DDSM

First, we will conduct all experiments using the CBIS-DDSM dataset, which consists of low-quality digitized analog mammograms. All images were resized to 1152×896 pixels before processing. The CBIS-DDSM dataset was used in its entirety, preserving its original division into training and test sets, as shown in Table I.

Each network was trained three times. For patch classifiers, we evaluated accuracy, while for full-image classifiers, we measured the Area Under the Curve (AUC). From each training round, we selected the model with the highest performance on the validation set and evaluated it on the test set, recording this result as “Best Test.” We also calculated “Test Mean,” the average performance across the three models, along with its standard deviation. The standard error of the AUC for “Best Test” was computed using the Hanley and McNeil method [16] in a single run.

<sup>1</sup><https://pytorch.org/vision/stable/models.html>

<sup>2</sup><https://github.com/dpetrini/multiple-view>

TABLE I  
DIVISION OF CBIS-DDSM DATASET INTO TRAINING, VALIDATION, AND TEST SETS.

Type	Training	Validation	Test
Mammograms	2,212	246	645

#### A. Single View Classifiers

1) *Patch Classifier and Base-Model:* In this section, we aim to address questions (1) and (2) outlined in Section III. To investigate these, we perform two sets of experiments using different approaches to initialize the weights of single-view classifiers:

- 1) *Patch-Based Classifier (PBC):* Train a patch classifier and leverage transfer learning from its weights.
- 2) *Direct Classifier (DC):* Apply transfer learning directly from weights pre-trained on ImageNet.
- 2) *Patch Classifier:* Patches are 224×224 pixel fragments extracted from mammograms. In the CBIS-DDSM dataset, a patch classifier assigns each patch to one of five categories: background, benign calcification, malignant calcification, benign mass, or malignant mass. For every lesion, we generated 10 patches by randomly shifting the center of mass within a  $\pm 10\%$  range in various directions. Additionally, we extracted 10 background patches per image to ensure balanced representation.

The patch classifier is initialized with weights pre-trained on ImageNet and trained using the Adam optimizer, starting with an initial learning rate of  $2 \times 10^{-5}$ . The learning rate follows a “warm-up and cyclic cosine” schedule, configured with a period of 3, a maximum learning rate delta of  $2 \times 10^{-4}$ , and a warm-up phase lasting 4 epochs. The results, summarized in Table II, demonstrate that among the evaluated base models, ConvNeXt-Base achieves the highest performance.

3) *Patch Based Classifier (PBC):* We trained the models to classify single-view mammograms by leveraging the patch classifier weights obtained in the previous section and taking advantage of the fully convolutional network architecture, which enables the classification of images with varying sizes. To adapt the architecture for this task, we added two EfficientNet MBConv blocks (with stride=2) as the top layers, followed by a fully connected layer.

The resulting AUCs are presented in Table III. Notably, we observed that the best-performing base models for patch classification did not consistently perform well for full mammogram classification. Specifically, while ConvNeXt-Base was the top-performing model for patch classification, EfficientNet-B3 emerged as the best base model for classifying whole single-view mammograms.

4) *Direct Classifier (DC):* We trained the single-view classifiers using transfer learning directly from base models pre-trained on ImageNet, bypassing the patch classifier. The resulting AUCs are summarized in Table IV. Consistent with previous findings, EfficientNet-B3 achieved the best performance among the evaluated base models.

5) *Conclusions about Patch Classifier:* Comparing Tables III and IV, we observe that PBC and DC exhibit similar performance. Both approaches achieved their best results using the

TABLE II  
ACCURACY OF PATCH CLASSIFIERS. MODELS PRE-TRAINED ON  
IMAGENET-21K OR -22K ARE EXPLICITLY MARKED, WHILE THOSE  
TRAINED ON IMAGENET-1K ARE UNMARKED.

Model	Batch Size	Test mean	Best test
ViT-Base-CLIP-Laion-32	56	0.6464±0.0109	0.6487
MNASNet-1.0	144	0.6901±0.0269	0.7152
MobileNetV2	192	0.7391±0.0039	0.7369
EfficientNetV2-S (21k)	56	0.7524±0.0056	0.7460
MobileNetV3-Large	96	0.7357±0.0100	0.7462
EfficientNet-B1	192	0.7585±0.0090	0.7495
DenseNet169	144	0.7594±0.0053	0.7540
ResNet-18	192	0.7508±0.0075	0.7579
ResNeXt-50-32x4d	144	0.7580±0.0051	0.7585
DenseNet201	96	0.7617±0.0014	0.7604
EfficientNet-B0	192	0.7585±0.0035	0.7609
EfficientNet-B2	192	0.7550±0.0077	0.7637
EfficientNetV2-M	96	0.7501±0.0129	0.7641
ResNet-101	144	0.7574±0.0087	0.7644
ResNet-50	192	0.7550±0.0087	0.7650
EfficientNet-B4	96	0.7639±0.0057	0.7666
ConvNeXt-Base (22k)	96	0.7740±0.0063	0.7680
DenseNet121	144	0.7685±0.0119	0.7691
EfficientNetV2-S	96	0.7643±0.0111	0.7695
SwinV2-Base-In22k-FT-1k (22k)	56	0.7725±0.0048	0.7695
EfficientNet-B3	144	0.7661±0.0050	0.7700
ConvNeXt-Tiny	96	0.7711±0.0051	0.7721
ConvNeXt-Small	96	0.7791±0.0081	0.7784
ConvNeXt-Base	96	0.7831±0.0082	<b>0.7918</b>

EfficientNet-B3 network, with AUC values of  $0.8325 \pm 0.0171$  for PBC and  $0.8313 \pm 0.0172$  for DC — both very close (Table V).

To further analyze these results, we performed a hypothesis test<sup>3</sup> and obtained a  $p$ -value of 0.4721. This result suggests that a patch-based classifier (PBC) does not offer a significant advantage over directly utilizing ImageNet-pretrained weights (DC). Moreover, when Test Time Augmentation (TTA) was applied, DC demonstrated slightly superior performance compared to PBC. Additionally, while fourteen base models performed better under the PBC approach, eight showed improved results with DC. These findings further reinforce the conclusion that there is no clear benefit to using PBC over DC.

Thus, we can answer question (1): since PBC is more complex and time-consuming to train than DC, we conclude that pretraining on patches is not a suitable strategy for building classifiers for lower-quality mammography datasets such as CBIS-DDSM.

6) *Conclusions about Base-Models*: In this section, we analyze Tables III and IV to address the question (2), concluding:

- *EfficientNet-B3 consistently outperformed other models* on both PBC and DC approaches, making it the recommended base model for this task.
- *ImageNet-22k or -21k initializations did not significantly outperform ImageNet-1k initializations* for ConvNeXt and EfficientNetV2-S networks.

<sup>3</sup>In this test, we computed the standard errors  $SE_1$  and  $SE_2$  of the AUCs using the Hanley and McNeil formula [17]. We then calculated  $z = \frac{AUC_1 - AUC_2}{SE_{diff}}$ , where  $SE_{diff} = \sqrt{SE_1^2 + SE_2^2 - 2 \cdot r \cdot SE_1 \cdot SE_2}$ , assuming a Kendall-style correlation of  $r = 0.5$ .

TABLE III  
AUCs OBTAINED BY SINGLE-VIEW PATCH-BASED CLASSIFIERS (PBC).  
PBC/DC INDICATES WHICH APPROACH GENERATES THE HIGHEST AUC  
IN THE BEST TEST, COMPARING WITH TABLE IV. “TRAIN SIZE”  
INDICATES THE RESOLUTION OF THE TRAINING IMAGES OF THE BASE  
MODEL.

Model	Train size	Test mean	Best test	PBC /DC
MobileNetV3-Large	224	0.7426±0.0065	0.7353±0.0205	DC
MobileNetV2	224	0.7504±0.0315	0.7611±0.0198	DC
ResNet-50	224	0.7541±0.0207	0.7616±0.0197	DC
ResNeXt-50-32x4d	224	0.7705±0.0068	0.7627±0.0197	PBC
DenseNet121	224	0.7804±0.0161	0.7633±0.0197	PBC
MNASNet-1.0	224	0.7627±0.0066	0.7643±0.0197	PBC
EfficientNet-B4	384	0.7866±0.0040	0.7814±0.0191	DC
ConvNeXt-Tiny	224	0.7969±0.0102	0.7850±0.0190	PBC
ResNet-18	224	0.7749±0.0129	0.7858±0.0189	PBC
EfficientNetV2-S	300	0.8034±0.0117	0.7886±0.0189	DC
DenseNet201	224	0.7884±0.0129	0.7891±0.0188	PBC
ResNet-101	224	0.7791±0.0093	0.7892±0.0188	PBC
EfficientNet-B0	224	0.7933±0.0096	0.7977±0.0185	DC
ConvNeXt-Small	224	0.8010±0.0033	0.7984±0.0185	PBC
ConvNeXt-Base	224	0.7991±0.0045	0.8019±0.0184	PBC
ConvNeXt-Base (22k)	224	0.8137±0.0108	0.8027±0.0183	PBC
EfficientNet-B2	260	0.8054±0.0128	0.8120±0.0180	PBC
DenseNet169	224	0.7910±0.0106	0.8031±0.0183	PBC
EfficientNet-B1	240	0.7884±0.0120	0.8054±0.0182	DC
EfficientNetV2-S (21k)	300	0.8089±0.0052	0.8114±0.0180	DC
EfficientNetV2-M	384	0.7931±0.0158	0.8150±0.0179	PBC
EfficientNet-B3	300	0.8114±0.0153	<b>0.8325±0.0171</b>	PBC

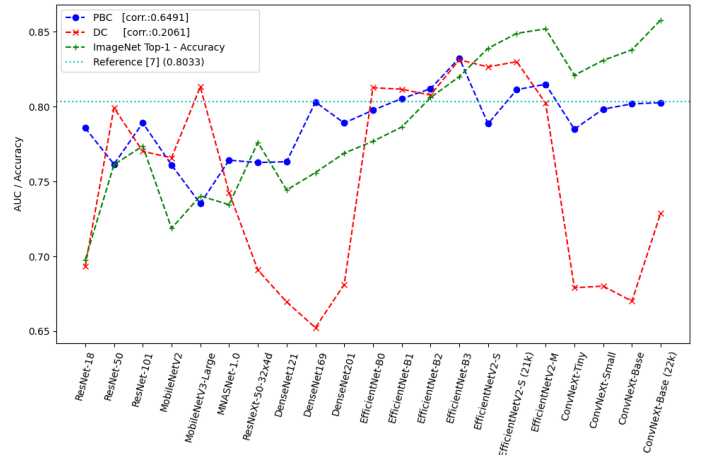


Fig. 1. AUC values for all single-view PBC and DC classifiers on the CBIS-DDSM dataset, along with the accuracies of their backbone models on ImageNet classification, and the corresponding Pearson correlation coefficients.

- *Larger training image sizes (300×300 or greater)* were associated with the best-performing networks for both PBC (Table III) and DC (Table IV).
- *Correlation analysis between base model performance and classifier performance* is illustrated in Fig. 1. We computed the Pearson correlation coefficient ( $r$ ) between the AUCs of PBCs and the top-1 accuracy of their base models on ImageNet, yielding  $r = 0.65$ , indicating a moderate positive correlation. This suggests that PBCs generally benefit from stronger base models. In contrast, DC classifiers showed a weak correlation ( $r = 0.21$ ), implying that their performance is less dependent on the base model’s ImageNet accuracy.

TABLE IV

AUCs OBTAINED BY SINGLE-VIEW DIRECT CLASSIFIERS (DC). PBC/DC INDICATES WHICH APPROACH GENERATES THE HIGHEST AUC IN THE BEST TEST, COMPARING WITH TABLE III. "TRAIN SIZE" INDICATES THE RESOLUTION OF THE TRAINING IMAGES OF THE BASE MODEL.

Model	Train size	Test mean	Best test	PBC /DC
DenseNet169	224	0.6784±0.0184	0.6524±0.0222	PBC
DenseNet121	224	0.6697±0.0057	0.6696±0.0219	PBC
ConvNeXt-Base	224	0.6817±0.0178	0.6701±0.0219	PBC
ConvNeXt-Tiny	224	0.6889±0.0123	0.6791±0.0218	PBC
ConvNeXt-Small	224	0.6674±0.0152	0.6802±0.0217	PBC
DenseNet201	224	0.6878±0.0078	0.6812±0.0217	PBC
ResNeXt-50-32x4d	224	0.6876±0.0054	0.6909±0.0215	PBC
ResNet-18	224	0.6883±0.0073	0.6935±0.0215	PBC
ConvNeXt-Base (22k)	224	0.7019±0.0262	0.7289±0.0207	PBC
MNASNet-1.0	224	0.7633±0.0147	0.7427±0.0203	PBC
MobileNetV2	224	0.7584±0.0251	0.7659±0.0196	DC
ResNet-101	224	0.7698±0.0092	0.7702±0.0195	PBC
EfficientNet-B4	384	0.8023±0.0064	0.7933±0.0187	DC
ResNet-50	224	0.7293±0.0598	0.7993±0.0185	DC
EfficientNetV2-M	384	0.7605±0.0376	0.8024±0.0183	PBC
EfficientNet-B2	260	0.8058±0.0071	0.8078±0.0181	PBC
EfficientNet-B1	240	0.8023±0.0156	0.8117±0.0180	DC
EfficientNet-B0	224	0.7691±0.0525	0.8127±0.0179	DC
MobileNetV3-Large	224	0.7792±0.0247	0.8132±0.0179	DC
EfficientNetV2-S	300	0.8100±0.0251	0.8266±0.0174	DC
EfficientNetV2-S (21k)	300	0.8098±0.0162	0.8301±0.0172	DC
EfficientNet-B3	300	0.8087±0.0177	<b>0.8313±0.0172</b>	PBC

TABLE V

AUCs OF THE BEST-PERFORMING SINGLE-VIEW CLASSIFIERS ON THE CBIS-DDSM DATASET.

Classifier	Network	Result	TTA
Reference [7]	EfficientNet-B0	0.8033±0.0183	0.8153±0.0178
PBC	EfficientNet-B3	<b>0.8325±0.0171</b>	0.8343±0.0170
DC	EfficientNet-B3	0.8313±0.0172	<b>0.8358±0.0170</b>

7) *Comparison with Previous Work*: The AUCs achieved by our patch-based classifier (PBC – 0.8325) and direct classifier (DC – 0.8313) are significantly higher than the best result reported in [7] (0.8033). Using the hypothesis test described on page 3, we compared the AUC of our PBC model with the previous work, obtaining a p-value of 0.0499. Similarly, the comparison for our DC model yielded a p-value of 0.0575. These results demonstrate that the improvements in our work are substantial, with some statistical significance. We attribute these gains to the use of modern pre-training strategies for ImageNet-based models. For instance, He et al. [18] improved the top-1 accuracy of ResNet50 from 75.3% to 79.29%, with 2.13% of this improvement directly attributable to advanced techniques such as cosine learning rate decay, label smoothing, and Mixup. Further enhancements by Wightman et al. [19] increased this accuracy to 80.4% through the incorporation of the LAMB optimizer and CutMix augmentation.

In the Test Time Augmentation (TTA) experiments, the direct classifier (DC) in this study achieved an AUC of 0.8343, compared to the AUC of 0.8153 reported in [7].

### B. Classifiers with Resized Images

To address question (3) outlined in Section III, we tested reducing the input image size by half, resulting in dimensions

of 576×448. We conducted two experiments using different downsampling methods. The first experiment employed conventional interpolation, while the second utilized a machine learning-based downsampling technique called “Learn to Resize” [11]. If this technique demonstrates superior performance compared to conventional resampling, it could become the preferred method for reducing high-resolution mammograms to a resolution compatible with current processing devices.

1) *Fixed Resizing Classifier (FRC)*: We downsampled the original 1152×892 images to 576×448 using the INTER\_AREA interpolation method from the OpenCV library. Transfer learning was then performed directly from the ImageNet pre-trained weights. The results, presented in Table VI, show that the highest AUC achieved was 0.8167±0.0178. This performance is notably lower than the results obtained without downsampling: 0.8313±0.0172 for direct classification (DC).

TABLE VI

AUCs OF SINGLE-VIEW DIRECT CLASSIFIERS USING FIXED RESIZING (FRC).

Model	Train size	Test mean	Best test
MNASNet-1.0	224	0.5643±0.0267	0.5860±0.0230
MobileNetV2	224	0.6858±0.0169	0.6972±0.0214
ConvNeXt-Small	224	0.7084±0.0240	0.7117±0.0211
ConvNeXt-Tiny	224	0.7118±0.0330	0.7214±0.0209
ResNet-18	224	0.7433±0.0274	0.7536±0.0200
EfficientNet-B2	260	0.7622±0.0143	0.7656±0.0196
EfficientNet-B1	240	0.7644±0.0077	0.7680±0.0195
DenseNet121	224	0.7896±0.0106	0.7751±0.0193
MobileNetV3-Large	224	0.7811±0.0131	0.7753±0.0193
EfficientNetV2-S (21k)	300	0.7808±0.0071	0.7761±0.0193
EfficientNetV2-M	384	0.7723±0.0269	0.7832±0.0190
ResNeXt-50-32x4d	224	0.7817±0.0137	0.7881±0.0189
EfficientNet-B4	384	0.7847±0.0053	0.7890±0.0188
DenseNet201	224	0.7813±0.0107	0.7943±0.0186
EfficientNet-B0	224	0.7686±0.0242	0.7956±0.0186
ConvNeXt-Base (22k)	224	0.7951±0.0057	0.7958±0.0186
DenseNet169	224	0.7795±0.0124	0.7968±0.0186
EfficientNet-B3	300	0.8010±0.0175	0.7972±0.0185
ResNet-101	224	0.7876±0.0207	0.7981±0.0185
ConvNeXt-Base	224	0.7423±0.0440	0.8009±0.0184
EfficientNetV2-S	300	0.7901±0.0102	0.8049±0.0183
ResNet-50	224	0.7756±0.0300	<b>0.8167±0.0178</b>

2) *Learn-to-Resize Classifier (LRC)*: Talebi and Milanfar [11] proposed a technique called “Learn to Resize,” which integrates bilinear resizing with convolutional layers, enabling the model to optimize resizing for improved classification performance. As shown in Table VII, the highest AUC achieved using this method was 0.7958±0.0186, which is lower than the results obtained with fixed resizing (FRC).

3) *Conclusions on Resizing*: Table VIII summarizes the highest AUCs obtained with and without resizing. They show that the “Learn to Resize” technique (LRC) underperformed compared to fixed resizing (FRC), despite its greater complexity, suggesting that while LRC is effective for reducing the resolution of natural images, it is not well-suited for mammograms. Additionally, downscaling the input images led to a significant decrease in AUC.

Hypothesis test described on page 3 reveals that patch-based classification (PBC) is significantly superior to LRC, with a p-

TABLE VII  
AUCs OF SINGLE-VIEW DIRECT CLASSIFIERS WITH LEARNED RESIZING (LRC).

Model	Train size	Test mean	Best test
DenseNet121	224	0.6712±0.0208	0.6518±0.0222
ResNeXt-50-32x4d	224	0.6735±0.0042	0.6682±0.0220
ConvNeXt-Small	224	0.6734±0.0080	0.6709±0.0219
DenseNet169	224	0.6718±0.0178	0.6850±0.0216
DenseNet201	224	0.6848±0.0018	0.6855±0.0216
ResNet-18	224	0.6847±0.0030	0.6884±0.0216
ConvNeXt-Base	224	0.6791±0.0076	0.6892±0.0216
EfficientNet-B4	384	0.7501±0.0274	0.7113±0.0211
EfficientNet-B0	224	0.7494±0.0228	0.7174±0.0209
ResNet-50	224	0.7188±0.0082	0.7272±0.0207
MobileNetV2	224	0.7096±0.0269	0.7297±0.0206
ResNet-101	224	0.7230±0.0226	0.7532±0.0200
EfficientNet-B1	240	0.7477±0.0063	0.7547±0.0200
EfficientNet-B3	300	0.7613±0.0094	0.7564±0.0199
ConvNeXt-Tiny	224	0.7200±0.0273	0.7574±0.0199
MNASNet-1.0	224	0.6979±0.0464	0.7626±0.0197
EfficientNet-B2	260	0.7497±0.0345	0.7690±0.0195
ConvNeXt-Base (22k)	224	0.7399±0.0393	0.7707±0.0195
EfficientNetV2-M	384	0.7335±0.0297	0.7749±0.0193
EfficientNetV2-S (21k)	300	0.7719±0.0122	0.7779±0.0192
EfficientNetV2-S	300	0.7475±0.0342	0.7890±0.0188
MobileNetV3-Large	224	0.7724±0.0194	<b>0.7958±0.0186</b>

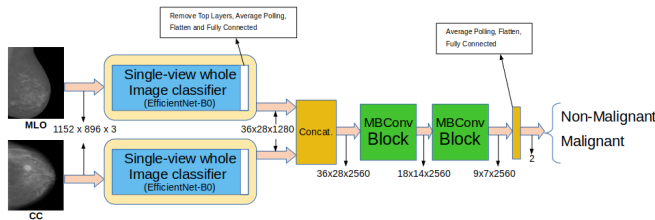


Fig. 2. Two-view classifier with EfficientNet-B0 backbone.

value of 0.0202. However, there is limited statistical evidence to conclude that PBC outperforms FRC, as the p-value for this comparison is 0.1828.

From Tables VI and VII, we observed that the best-performing networks using FRC and LRC utilized base models pre-trained on small image sizes of 224×224.

TABLE VIII  
AUCs OF SINGLE VIEW CLASSIFIERS WITH AND WITHOUT RESIZING.

Classifier	Best network	Result
FRC (with resizing)	ResNet-50	0.8167±0.0178
LRC (with resizing)	MobileNetV3_Large	0.7958±0.0186
PBC (without resizing)	EfficientNet-B3	<b>0.8325±0.0171</b>
DC (without resizing)	EfficientNet-B3	0.8313±0.0172

### C. Two-View Classifier

In this section, we aim to address the question (4) listed in Section III.

1) *Architecture of Two-View Classifier*: We assembled the network as in Fig. 2 making another transfer learning with the weights obtained from the best single-view models of section IV-A. We obtained the AUCs described in Table IX.

The best two-view classifier was achieved using the direct classification (DC) approach with the EfficientNet-B3 base model, yielding an AUC of 0.8643. This represents the highest AUC recorded for classifying two-view exams in the CBIS-DDSM dataset under its original training/testing split. This result surpasses the AUC of 0.8418 reported in [7] using EfficientNet-B0, with some statistical evidence of superiority (p-value = 0.0821, using hypothesis test described on page 3). We attribute this improvement to the use of a base model trained with more advanced and modern techniques, as discussed in Section IV-A.5. Using Test Time Augmentation (TTA), we achieved an AUC of 0.8658, compared to the AUC of 0.8483 reported in [7]. The hypothesis test yielded a p-value of 0.1366, indicating weak statistical evidence that our result is superior to the previous.

TABLE IX  
AUCs OF THE TOP-PERFORMING TWO-VIEW CLASSIFIERS, BUILT USING THE BEST SINGLE-VIEW CLASSIFIERS.

Model	Test mean	Best test	TTA
EfficientNet-B3 (PBC)	0.8523±0.0073	0.8468±0.0254	0.8490±0.0253
EfficientNet-B3 (DC)	0.8605±0.0028	<b>0.8643±0.0241</b>	<b>0.8658±0.0239</b>

2) *Average or Maximum Operation*: The results of two-view and single-view classifiers cannot be directly compared, as they involve different numbers of test cases. So, we compared the best two-view result from the Table IX with the result obtained by making inferences independently for each view (CC and MLO) and calculating the average or maximum of the two probabilities.

TABLE X  
AUC OF THE TWO-VIEW MODEL COMPARED TO THE AUCs OBTAINED BY PROCESSING THE CC AND MLO VIEWS INDEPENDENTLY AND COMBINING THEIR OUTPUTS USING MEAN OR MAXIMUM OPERATIONS.

Model	Two-view model	Mean	Maximum
EfficientNet-B3 (DC)	<b>0.8643±0.0241</b>	0.8420±0.0257	0.8426±0.0257

We conducted the DeLong test<sup>4</sup> to compare the two-view model with the mean and maximum operations (Table X). The resulting p-values were 0.0280 and 0.0286, respectively.

We can now address question (4): classifying two views simultaneously is statistically superior to classifying individual views and combining their results using mean or maximum operations. This improvement likely stems from the fact that concatenated views provide additional information, such as the spatial locations of lesions, which is not captured by simply aggregating the outputs of separate views.

## V. ARCHITECTURE EXPLORATION IN VINDR-MAMMO

In this section, we will repeat the experiments using the VinDr-Mammo dataset, which consists entirely of Full-Field Digital Mammographies (FFDMs), to answer the question (5) listed in Section III. Unlike CBIS-DDSM, this dataset does not

<sup>4</sup>An AUC comparison method developed by DeLong et al. [20]. We used the one-tailed fast version proposed by Sun, Xu, and Xu [21], with the implementation available at [https://github.com/yandexdataschool/roc\\_comparison](https://github.com/yandexdataschool/roc_comparison), computing the unadjusted AUC covariance.

include biopsy-confirmed benign or malignant labels. Instead, it provides Bi-RADS (Breast Imaging Reporting and Data System) and other annotations, uniformly distributed across 4,000 training exams and 1,000 test exams.

The distribution of Bi-RADS categories is: 1 (67.03%), 2 (23.38%), 3 (4.65%), 4 (3.81%), and 5 (1.13%). To evaluate the performance of full-image classifiers, we grouped the Bi-RADS categories into two broader classes: “Normal” for views classified as Bi-RADS 1 and 2, and “Abnormal” for views classified as Bi-RADS 3, 4, and 5. This grouping was based on the presence of lesion annotations in the latter categories. As a result, the “Abnormal” class represents approximately 10% of the dataset. We assessed the target task of categorizing mammograms into these two classes (Table XI).

TABLE XI  
NUMBER OF VINDR-MAMMO IMAGES USED IN THIS EXPERIMENT.

Type	Training	Validation	Test
Mammograms	14,394	1,604	4,000
Abnormal	1,380	154	384
Normal	13,014	1,450	3,616

To construct the patch dataset, outlined in Table XII, we utilized the lesion annotations provided in the VinDr-Mammo dataset.

TABLE XII  
NUMBER OF VINDR-MAMMO PATCHES USED IN THIS WORK.

Type	Training	Validation	Test
Bi-Rads 3	5,820	710	1,680
Bi-Rads 4	6,320	680	1,810
Bi-Rads 5	2,590	400	810
Background	13,567	1,647	3,963

### A. Single View Classifier

1) *Patch Classifier and Base-Model*: To answer questions (1) and (2) of Section III, we prepared the patches similar to Section IV-A.2, considering four categories: background and the lesions with Bi-Rads 3, 4 and 5. The backbone model with the best performance was ConvNeXt\_Base\_22k (Table XIII).

TABLE XIII  
CLASSIFICATION ACCURACIES OF THE PATCH CLASSIFIERS EVALUATED ON THE VINDR-MAMMO DATASET.

Model	Batch size	Test mean	Best test
MobileNetV2	384	0.6644±0.0071	0.6637
ResNet-50	384	0.6751±0.0130	0.6665
DenseNet169	384	0.6793±0.0104	0.6798
EfficientNetV2-S (21k)	384	0.6857±0.0099	0.6970
EfficientNet-B3	384	0.7002±0.0015	0.6991
EfficientNet-B0	384	0.6899±0.0092	0.7000
ConvNeXt-Base (22k)	256	0.6921±0.0133	<b>0.7052</b>

2) *Patch Based Classifier (PBC)*: Using the weights obtained from the patch classifier, we constructed single-view patch-based classification (PBC) models and achieved the results presented in Table XIV. Training the ConvNeXt-Base (22k) model required approximately 24 hours for the three rounds on an NVIDIA A100 GPU with 40 GB of memory,

making it the most time-intensive single-view model in this study.

TABLE XIV  
AUCS OF THE SINGLE-VIEW CLASSIFIER BASED ON PATCHES (PBC) FOR VINDR-MAMMO.

Model	Train size	Test mean	Best test	PBC /DC
MobileNetV2	224	0.6978±0.0086	0.6858±0.0216	DC
DenseNet169	224	0.8103±0.0140	0.7924±0.0187	DC
EfficientNetV2-S (21k)	300	0.8060±0.0089	0.7934±0.0187	DC
ResNet50	224	0.7797±0.0303	0.8005±0.0184	PBC
EfficientNet-B0	224	0.7986±0.0249	0.8208±0.0176	PBC
EfficientNet-B3	300	0.8172±0.0106	0.8280±0.0173	PBC
ConvNeXt-Base (22k)	224	0.8454±0.0086	<b>0.8510±0.0163</b>	PBC

3) *Direct Classifier (DC)*: The results of the Direct Classifier (DC) experiments are summarized in Table XV. DenseNet169 emerged as the top-performing base model. Notably, the best-performing Patch-Based Classifier (PBC), ConvNeXt\_Base\_22k, showed a significant drop in performance when applied to the DC approach. Conversely, DenseNet169, which excelled in the DC task, performed poorly in the PBC setting.

TABLE XV  
AUCS OF THE DIRECT SINGLE-VIEW CLASSIFIER (DC) FOR VINDR-MAMMO.

Model	Train size	Test mean	Best test	PBC /DC
ConvNeXt_Base (22k)	224	0.6567±0.0129	0.7367±0.0150	PBC
MobileNetV2	224	0.7734±0.0043	0.7653±0.0146	DC
ResNet50	224	0.7999±0.0042	0.7942±0.0140	PBC
EfficientNet-B3	300	0.8195±0.0092	0.8072±0.0137	PBC
EfficientNetV2-S (21k)	300	0.8084±0.0030	0.8074±0.0137	DC
EfficientNet-B0	224	0.8090±0.0067	0.8099±0.0136	PBC
DenseNet169	224	0.8045±0.0067	<b>0.8134±0.0136</b>	DC

4) *Conclusions about PBC*: We compared the best PBC result (ConvNeXt\_Base\_22k, 0.8510±0.0163, Table XIV) with the best DC result (DenseNet169, 0.8134±0.0136, Table XV) by running the DeLong test and obtained the value  $p = 0.0013$ . This indicates with statistical significance that the best PBC model is superior to the best DC model for classifying high-quality mammograms. Due to this result, we recommend the PBC approach for the VinDr-Mammo set with 100% digital mammograms, despite the fact that it requires more training time.

On the other hand, four base models performed better in the Patch-Based Classifier (PBC) approach, while three models showed superior performance in the Direct Classifier (DC) approach (see Fig. 3 and Tables XIV and XV). Based on these results, it is not possible to conclude that the PBC approach is universally superior to the DC approach for classifying high-quality mammograms, as performance varies depending on the base model.

5) *Conclusions on Base Models*: Fig. 3 provides a comparison between the performance of the base models in mammogram classification and their performance on ImageNet. The Patch-Based Classifier (PBC) approach exhibits a high correlation coefficient (0.7288), suggesting that its performance

closely aligns with the advancements in the evaluated networks. In contrast, the Direct Classifier (DC) approach showed a low negative correlation, indicating a lack of alignment with network improvements. These results suggest that the optimal strategy for classifying high-quality mammograms is to use a modern base model combined with the PBC approach.

### B. Classifiers with Resized Images

To answer the question (3) listed in Section III for VinDr-Mammo, we downsample mammograms to half their size before classifying them.

1) *Fixed Resizing Classifier (FRC)*: After resizing the images by half using OpenCV’s INTER\_AREA interpolation, we obtained the classification results presented in Table XVI.

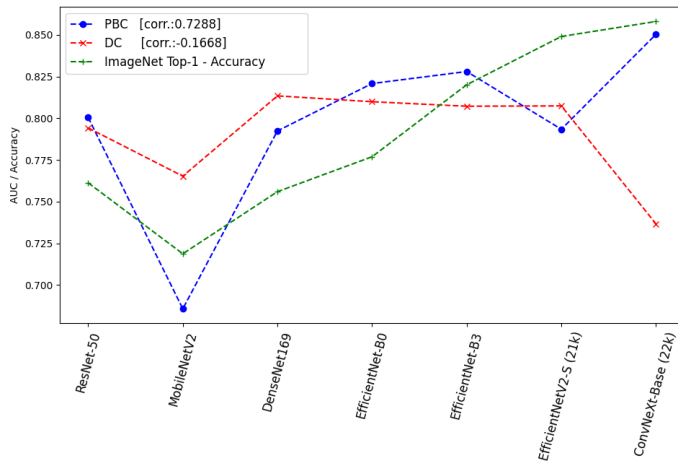


Fig. 3. The AUC scores for all single-view PBC and DC classifiers evaluated on the VinDr-Mammo dataset, accompanied by the ImageNet classification accuracies of their backbone models and the associated Pearson correlation coefficients.

TABLE XVI  
AUCs OF FIXED RESIZING CLASSIFIERS (FRCs) ON THE VINDR-MAMMO DATASET.

Model	Train size	Test average	Best test
MobileNetV2	224	0.7369±0.0168	0.7132±0.0153
EfficientNetV2-S (21k)	300	0.7948±0.0197	0.7691±0.0145
EfficientNet-B0	224	0.7795±0.0025	0.7815±0.0143
DenseNet169	224	0.7903±0.0037	0.7856±0.0142
ConvNeXt_Base (22k)	224	0.7642±0.0447	0.7869±0.0142
EfficientNet-B3	300	0.7963±0.0044	0.7978±0.0139
ResNet50	224	0.7916±0.0150	<b>0.8116±0.0136</b>

2) *Learn-to-Resize Classifier (LRC)*: After reducing the resolution of the mammograms by half using the “learn to resize” technique, we obtained the classification results presented in Table XVII.

3) *Conclusions on Resizing*: As in Section IV-B.3, the top-performing Learn-to-Resize Classifier (LRC) demonstrated inferior performance compared to the best Fixed Resizing Classifier (FRC). Since LRC is both computationally more complex and resource-intensive than FRC, the Learn-to-Resize approach offers no practical benefit.

TABLE XVII  
AUCs OF LEARN-TO-RESIZE CLASSIFIERS (LRCs) ON THE VINDR-MAMMO DATASET.

Model	Train size	Test average	Best test
ConvNeXt_Base (22k)	224	0.5654±0.0103	0.5750±0.0159
DenseNet169	224	0.6937±0.0945	0.7537±0.0148
EfficientNet-B0	224	0.7640±0.0112	0.7622±0.0146
ResNet50	224	0.7911±0.0172	0.7715±0.0145
EfficientNet-B3	300	0.7869±0.0074	0.7767±0.0144
MobileNetV2	224	0.7589±0.0276	0.7910±0.0141
EfficientNetV2-S (21k)	300	0.7891±0.0234	<b>0.8095±0.0137</b>

In addition, the best classifier with resolution reduction has a substantially lower AUC (576×448, 0.8116±0.0136) than the best classifier without resolution reduction (1152×892, 0.8510±0.0163). Therefore, it is not recommended to reduce the resolution of high-quality digital mammograms before classifying them. This suggests that using an even higher resolution (e.g., 2304×1792) is likely to improve performance.

### C. Two-View Classifier

To address question (4), we followed the same network creation and training process outlined in Section IV-C. We constructed a two-view classifier using the ConvNeXt\_Base\_22k network, initializing it with weights from the single-view PBC approach. Additionally, we processed each view (CC and MLO) individually using the best-performing classifier from the previous section (ConvNeXt\_Base\_22k) and combined the results using both average and maximum operations. The results are shown in Table XVIII.

TABLE XVIII  
AUCs OF THE TWO-VIEW MODEL COMPARED TO RESULTS OBTAINED BY AVERAGING AND TAKING THE MAXIMUM OF THE CC AND MLO VIEWS FROM THE SINGLE-VIEW MODEL.

Model	Two-View	Average	Maximum
ConvNext(PBC)	<b>0.8511±0.0177</b>	0.8019±0.0196	0.8017±0.0196

We compared the AUC of the two-view classifier with the AUCs obtained by calculating the mean and maximum of the CC and MLO outputs from the single-view classifier. Using the fast version of the DeLong test, we obtained p-values of  $p = 0.0030$  and  $p = 0.0025$ , respectively. These results provide strong statistical evidence that the two-view PBC classifier outperforms both the averaging and maximizing approaches applied to the outputs of the single-view classifier.

## VI. CONCLUSIONS

Single-view classifiers using PBC and DC approaches yielded very similar AUCs on the CBIS-DDSM dataset. Given that PBC is more complex and computationally intensive compared to DC, we recommend using ImageNet weights directly for classifying low-quality mammograms. On the VinDr-Mammo dataset, the PBC approach achieved a significantly higher AUC compared to DC. Therefore, despite the increased training time, we recommend PBC approach for building classifiers for high-quality mammograms.

We computed the Pearson correlation coefficients between the performance of the PBC and DC approaches and the base models' accuracies on ImageNet. The PBC approach showed moderately high correlations, suggesting that its performance improves with the use of more modern networks. In contrast, DC exhibited weak correlations, indicating that using modern base models does not provide significant benefits for this approach.

The best classification results for VinDr-Mammo were achieved using a modern network (ConvNeXt), whereas the top results for CBIS-DDSM were obtained with older networks (EfficientNet family). This suggests that the fine details in fully digital mammograms may necessitate more advanced base models for optimal performance.

The downsampled classifiers (576×448) produced lower AUCs compared to classifiers at the original resolution (1152×896) across both datasets and approaches. Therefore, we do not recommend reducing mammogram resolution by 50% prior to classification. In both datasets, the Fixed Resize Classifier (FRC) achieved higher AUCs than the Learn-to-Resize Classifier (LRC). Given that FRC is also less computationally demanding than LRC, there is no practical advantage to using the “learn to resize” approach.

For both sets, the two-view classifier was clearly superior to calculating the mean or maximum of the outputs of the CC and MLO individual views.

- [1] World Cancer Research Fund International WCRF. World cancer research fund international, 2024. Available at: <https://www.wcrf.org/dietandcancer/worldwide-cancer-data/>. Accessed on: Sept. 12, 2024.
- [2] L. Shen, L.R. Margolies, J. H. Rothstein, E. Fluder, R. McBride, and W. Sieh. Deep learning to improve breast cancer detection on screening mammography. *Scientific Reports*, 9(1):1–12, 2019.
- [3] X. Shu, L. Zhang, Z. Wang, Q. Lv, and Z. Yi. Deep neural networks with region-based pooling structures for mammographic image classification. *IEEE T. Medical Imaging*, 39(6):2246–2255, 2020.
- [4] T. Wei, Angelica I. A.-Rivero, S. Wang, Y. Huang, F. J. Gilbert, C.-B. Schönlieb, and C. W. Chen. Beyond fine-tuning: Classifying high resolution mammograms using function-preserving transformations. *arXiv:2101.07945*, 2021.
- [5] K. He, X. Zhang, S. Ren, and J. Sun. Deep residual learning for image recognition. In *Proc. IEEE Conf. Comp. Vision Patt. Recog.*, pages 770–778, 2016.
- [6] S. M. McKinney, M. Sieniek, V. Godbole, et al. International evaluation of an ai system for breast cancer screening. *Nature*, 577(7788):89–94, 2020.
- [7] D. G. P. Petrini, C. Shimizu, R. A. Roela, G. V. Valente, M. A. A. K. Fogueira, and H. Y. Kim. Breast cancer diagnosis in two-view mammography using end-to-end trained efficientnet-based convolutional network. *IEEE Access*, 10:77723–77731, 2022.
- [8] Y. Chen, H. Wang, C. Wang, Y. Tian, F. Liu, Y. Liu, M. Elliott, D. J. McCarthy, H. Frazer, and G. Carneiro. Multi-view local co-occurrence and global consistency learning improve mammogram classification generalisation. In *Int. Conf. Medical Image Comp. and Computer-Assisted Intervention*, pages 3–13. Springer, 2022.
- [9] T.-H. Nguyen, Q. H. Kha, T. N. T. Truong, B. T. Lam, B. H. Ngo, Q. V. Dinh, and N. Q. K. Le. Towards robust natural-looking mammography lesion synthesis on ipsilateral dual-views breast cancer analysis. In *IEEE/CVF Int. Conf. Computer Vision (ICCV) Workshops*, pages 2564–2573, Oct. 2023.
- [10] S. Sarker, P. Sarker, G. Bebis, and A. Tavakkoli. Mv-swin-t: mammogram classification with multi-view swin transformer. In *IEEE Int. Symp. on Biomedical Imaging (ISBI)*, pages 1–5. IEEE, 2024.
- [11] H. Talebi and P. Milanfar. Learning to resize images for computer vision tasks. In *IEEE/CVF Int. Conf. Computer Vision (ICCV)*, pages 487–496, 2021.
- [12] R. S. Lee, F. Gimenez, A. Hoogi, K. K. Miyake, M. Gorovoy, and D. L. Rubin. A curated mammography data set for use in computer-aided detection and diagnosis research. *Scientific Data*, 4(1):1–9, 2017.
- [13] H. T. Nguyen, H. Q. Nguyen, and H. H. Pham. Vindr-mammo: A large-scale benchmark dataset for computer-aided diagnosis in full-field digital mammography. *Scientific Data*, 10(277), 2023.
- [14] Z. Liu, H. Mao, C.-Y. Wu, C. Feichtenhofer, T. Darrell, and S. Xie. A convnet for the 2020s. *arXiv:2201.03545*, 2022.
- [15] R. Wightman. Pytorch image models, 2019. Available at: <https://github.com/rwightman/pytorch-image-models>. Accessed on: Jun. 6, 2024.
- [16] J. A. Hanley and B. J. McNeil. The meaning and use of the area under a receiver operating characteristic (roc) curve. *Radiology*, 143(1):29–36, 1982.
- [17] J. A. Hanley and B. J. McNeil. A method of comparing the areas under receiver operating characteristic curves derived from the same cases. *Radiology*, 148(3):839–843, 1983.
- [18] T. He, Z. Zhang, H. Zhang, Z. Zhang, J. Xie, and M. Li. Bag of tricks for image classification with convolutional neural networks. *arXiv:1812.01187*, 2018.
- [19] R. Wightman, H. Touvron, and H. Jégou. Resnet strikes back: An improved training procedure in timm. *arXiv:2110.00476*, 2021.
- [20] E. R. DeLong, D. M. DeLong, and D. L. Clarke-Pearson. Comparing the areas under two or more correlated receiver operating characteristic curves: a nonparametric approach. *Biometrics*, 44(3):837–845, 1988.
- [21] X. Sun and W. Xu. Fast implementation of delong’s algorithm for comparing the areas under correlated receiver operating characteristic curves. *IEEE Signal Processing Letters*, 21(11):1389–1393, 2014.